Published as: *Org Geochem*. 2013 March ; 56: 120–130.

Identification and quantification of polyfunctionalized hopanoids by high temperature gas chromatography–mass spectrometry

Alex L. Sessions[a,*], **Lichun Zhang**[a], **Paula V. Welander**[b], **David Doughty**[c,d], **Roger E. Summons**[b], and **Dianne K. Newman**[a,c,d]

[a]Division of Geological and Planetary Sciences, California Institute of Technology, Pasadena, CA, USA

[b]Department of Earth, Atmospheric and Planetary Sciences, Massachusetts Institute of Technology, Cambridge, MA, USA

[c]Division of Biology, California Institute of Technology, Pasadena, CA, USA

[d]Howard Hughes Medical Institute, California Institute of Technology, Pasadena, CA, USA

Abstract

Hopanoids are triterpenoids produced mainly by bacteria, are ubiquitous in the environment, and have many important applications as biological markers. A wide variety of related hopanoid structures exists, many of which are polyfunctionalized. These modifications render the hopanoids too involatile for conventional gas chromatography (GC) separation, so require either laborious oxidative cleavage of the functional groups or specialized high temperature (HT) columns. Here we describe the systematic evaluation and optimization of a HT-GC method for the analysis of polyfunctionalized hopanoids and their methylated homologs. Total lipid extracts are derivatized with acetic anhydride and no further treatment or workup is required. We show that acid or base hydrolysis to remove di- and triacylglycerides leads to degradation of several BHP structures. DB-XLB type columns can elute hopanoids up to bacteriohopane-tetrol at 350 °C, with baseline separation of all 2-methyl/desmethyl homologs. DB-5HT type columns can additionally elute bacteriohopaneaminotriol and bacteriohopaneaminotetrol, but do not fully separate 2-methyl/desmethyl homologs. The method gave 2- to 7-fold higher recovery of hopanoids than oxidative cleavage and can provide accurate quantification of all analytes including 2-methyl hopanoids. By comparing data from mass spectra with those from a flame ionization detector, we show that the mass spectromet (MS) response factors for different hopanoids using either total ion counts or *m/z* 191 vary substantially. Similarly, 2-methyl ratios estimated from selected-ion data are lower than those from FID by 10–30% for most hopanoids, but higher by ca. 10% for bacteriohopanetetrol. Mass spectra for a broad suite of hopanoids, including 2-methyl homologs, from *Rhodopseudomonas palustris* are presented, together with the tentative assignment of several new hopanoid degradation products.

*Corresponding author. Tel.: +1 626 395 6445; fax: +1 626 683 0621. als@gps.caltech.edu (A.L. Sessions).

1. Introduction

Hopanoids are a distinctive class of pentacyclic triterpenoid lipids with wide ranging biogeochemical utility (Ourisson et al., 1979; Rohmer et al., 1984; Brocks et al., 2003). They are biosynthesized primarily by bacteria via cyclization of squalene to yield the C_{30} hydrocarbon, diploptene [hop-22(29)-ene; Ochs et al., 1992; Wendt et al., 1997,1999]. Subsequent enzymatic addition of a variety of functionalized small molecules can then yield hopanoids with side chains 5–9 carbons in length and with differing – and usually multiple – functional groups (Flesch and Rohmer, 1988; Kannenberg and Poralla, 1999). The products are known generically as bacteriohopanepolyols (BHPs), or hopanoids, and the menagerie of identified BHPs has grown to include those with amino, ether, nucleotide and cyclic sugar moieties, many of which appear to show specific organismal and environmental associations (Rohmer et al., 1984; Farrimond et al., 2000, 2004; Talbot and Farrimond, 2007). The tetrahydroxy compound bacteriohopanetetrol (BHtetrol) is generally the most abundant triterpenoid in many species. During diagenesis, BHPs are reduced and defunctionalized to yield a regular series of hopanes, commonly ranging from C_{28} to C_{35}, more rarely to higher carbon numbers, and with systematic stereochemical variation (Ourisson et al., 1979; Ourisson and Albrecht, 1992).

As a class, hopanoids have received attention from geochemists in a variety of roles. In modern sediments, functionalized BHPs are being explored as diagnostic for varying clades of bacteria (reviewed by Talbot and Farrimond (2007)).In rocks and oils,the relative abundance of different hopane isomers can provide information about both environmental conditions during deposition, as well as maturity (Seifert and Moldowan, 1980; Brassell et al., 1983; Peters and Moldowan, 1991; Peters et al., 2005). For ancient rocks, hopanoids methylated at C-2 or C-3 have received particular attention because they have been proposed as diagnostic markers for cyanobacteria and aerobic methylotrophs, respectively (Zundel and Rohmer, 1985a,b; Summons and Jahnke, 1990; Summons et al., 1994, 1999; Farrimond et al., 2004).A current research focus lies in understanding the cellular function of BHPs in bacteria, the genetic basis for their biosynthesis and modification, and their distribution and evolutionary relationships among extant organisms (Fischer et al., 2005; Blumenberg et al., 2006; Fischer and Pearson, 2007; Rashby et al., 2007; Doughty et al., 2009; Welander et al., 2009, 2010, 2012; Bradley et al., 2010).

A key component of all such investigations is the identification and quantification of hopanes and BHPs. Hopanes, hopenes, and diplopterol (the C_{30} hopanol) are readily analyzed using gas chromatography–mass spectrometry (GC–MS) and GC–MS-MS. However, polyfunctionalized BHPs are often too involatile for analysis via GC–MS using conventional columns. The most common alternative is to cleave the BHP polar side chain using H_5IO_6, followed by reduction with $NaBH_4$ or $LiEt_3BH$ (super hydride) to yield a C_{31} to C_{33} hopanol with only one OH (Rohmer et al., 1984; Rohmer, 2010). The procedure converts all functionalized BHPs to just a few hopanol skeletons that can be readily quantified via GC–MS. However, information encoded in the polar side chain is obviously lost and the procedure is time consuming. As an alternative, liquid chromatography–MS (LC–MS) using atmospheric pressure chemical ionization (APCI) has proven to give excellent results for polyfunctionalized BHPs with minimal sample preparation (Talbot et al., 2001). However, accurate quantitation of BHPs with this method is problematic because authentic standards of most functionalized hopanoids are not available. Current LC–MS techniques also provide poor sensitivity to hopanoid hydrocarbons (hopenes and hopanes).

Innes et al. (1997) reported that bacteriohopanetetrol (BHtetrol), derivatized as the tetraacetate, could be eluted from a 15 m DB-5HT GC column, but with incomplete separation of the 2-methyl and desmethyl homologs. Further work by Talbot et al. (2003c)

and Blumenberg et al. (2006) showed that bacteriohopanepentol (BHpentol) and bacteriohopaneaminotriol (BHaminotriol) would both also elute from this same column. Here, we extend those earlier efforts and describe in detail an optimized high temperature GC–MS method using newer capillary columns. We evaluate several alternative columns and show that the DB-XLB stationary phase can provide baseline separation of 2-methyl and desmethyl BHP homologs. We further compare quantitation of hopanoids using flame ionization detection (FID) peak areas, with total ion current (TIC) and single ion monitoring (SIM) peak areas from GC–MS, and using TIC peak areas from LC–MS to assess potential bias in quantitation. The capabilities of the new GC–MS method are demonstrated using *Rhodopseudomonas palustris*, a phototrophic bacterium that synthesizes a variety of hopanoids structures, including the 2-methyl homologs.

2. Methods

2.1. Samples

R. palustris strains TIE-1, DSM-123, CGA009, BisA53, BisB5, BisB18 and HaA2 were grown under anaerobic photoautotrophic, anaerobic photoheterotrophic, or aerobic heterotrophic conditions in 1 l batch cultures. A variety of strains and conditions were employed to produce extracts that varied in relative abundance and structure of BHPs, to allow us to more fully evaluate methodological limitations. For phototrophic growth, anaerobic carbonate-buffered freshwater medium (FW) was prepared by autoclaving 1 l of FW basal medium (5.6 mM NH_4Cl,3.7 mM KH_2PO_4,0.7 mM $CaCl_2$,2.0 mM $MgSO_4$) for 45 min and then allowing the mixture to cool under flowing N_2/CO_2. The following supplements were added from sterile stocks: 22 ml of 1 M $NaHCO_3$, 1 ml of 0.1 mg/ml Vitamin B_{12}, 1 ml trace elements [8.1 μM ethylenediaminetetraacetic acid (EDTA)], 4.0 μM $FeSO_4$,0.8 μM $CoCl_2$, 0.31 μM $ZnCl_2$,0.10 μM $NiCl_2$, 0.074 μM MoO_4, 4.8 μM H_3BO_3, 0.01 μM $CuCl_2$, 0.25 μM $MnCl_2$), 10 ml vitamin solution (0.29 μM 4-aminobenzoic acid, 41 nM D+-biotin, 0.81 μM nicotinic acid, 0.21 μM pantothenate, 0.41 μM pyridoxamine, 0.29 μM thiaminium, 1.32 μM riboflavin) and 2 ml of either 1 M thiosulfate (photoautotrophic) or 1 M sodium acetate (photoheterotrophic). The pH was measured after addition of supplements and adjusted with Na_2CO_3 to 6.8 as necessary. All anaerobic cultures were flushed and pressurized to 34 kPa with N_2/CO_2 (80/20) after inoculation and incubated at 30 °C with artificial illumination at 50 W/m^2 without shaking. Heterotrophic cultures were grown in unbuffered YP medium (0.3% yeast extract, 0.3% peptone), with shaking at 250 rpm in the dark at 30 °C. Biomass was harvested either at mid-log or stationary phase. Harvested cultures were pelleted by centrifugation at 5000 g for 20 min and were then lyophilized in a Virtis K-series freeze dryer. They were stored and transported frozen prior to extraction.

2.2. Sample workup

Dried biomass (typically ca. 30 mg) was extracted by shaking with 10 ml 1:2:0.9 dichloromethane(DCM):MeOH:water, followed by addition of equal volumes of water and DCM (Bligh and Dyer, 1959). The mixture was centrifuged at ca. 1500 rpm for 10–30 min to help separate the emulsion that typically developed. The organic phase was collected via pipette and filtered through combusted glass wool as necessary. The total lipid extract (TLE) was collected in a tared vial, dried and weighed, resuspended in DCM and one or more 0.5 mg aliquots were transferred to clean vials for further processing.

Two separate procedures were used to liberate BHPs and derivatize them for GC–MS. The first followed the procedure of Rohmer (2010) in which hopanoids are oxidatively cleaved between gemdiol functions and then reduced to yield C_{31} or C_{32} alcohols from penta and tetrafunctionalized BHPs, respectively. In this procedure, extracts were reacted with 300 mg

H_5IO_6 in 8:1 tetrahydrofuran (THF):water (3 ml) for 1 h at room temperature. Lipids were recovered by extraction (3×) with methyl *t*-butyl ether (MTBE), dried over anhydrous Na_2SO_4 and reduced with $NaBH_4$ (100 mg) in MeOH (3 ml) for 4 h at room temperature. Hopanol products were separated from other compounds (mainly fatty acids and aldehydes) with solid phase extraction on 0.5 g Sepra-NH_2 (Phenomenex) columns, with elution of the hopanols in 7 ml 9:1 DCM:acetone. They were derivatized to acetates by reaction with 1:1 acetic anhydride (Ac_2O):pyridine (0.2 ml,20 min, 70 °C) and the mixture injected into the gas chromatograph. We have not observed any significant detrimental effects to the GC–MS system when injecting this mixture.

The second procedure involved simply reacting the (dried) TLE with 1:1 Ac_2O:pyridine (100 μl; 70 °C, 20 min). Variation in time and temperature were also tested, as discussed in Section 3. Several samples were hydrolyzed with 20:1 anhydrous MeOH/AcCl to eliminate diacyl glycerides (this part of the procedure was later rejected, Section 3, due to degradation of some analytes). No further preparation of the extracts was required and they were injected in the reaction mixture into the GC instrument. Epiandrosterone (5α-androstan-3β-ol-17-one; 7 μg) was added to each sample as an internal standard immediately prior to injection, resulting in an injected concentration of ca. 70 ng/μl.

2.3. GC–MS

BHPs were analyzed using two separate GC–MS systems. The first, at the Massachusetts Institute of Technology (MIT), was an Agilent 7890 gas chromatograph attached to an Agilent 5975C mass selective detector equipped with a programmable temperature vaporization (PTV) injector. The second, at the California Institute of Technology (Caltech), was a Thermo Trace GC/DSQ instrument equipped with PTV injector and flame ionization detector (FID). With the latter instrument, the column effluent was split 4:1 between the mass spectrometer and FID to allow simultaneous quantification. Several columns were evaluated (Section 3), including DB-1HT, DB-5HT and DB-XLB (all Agilent Technologies). Columns were 30 m × 0.25 mm × 0.1 μm film thickness. The PTV injector was operated initially at 50 °C with 0.3 min hold (injection), ramped at 14 °/s to 125 °C with 1.0 min hold (solvent evaporation) and ramped at 14 °/s to 325 °C for the duration of the run (analyte transfer). The PTV injector was cleaned by heating to 360 °C in back flush for 3.0 min at the end of every run. The column oven program was: 100 °C (2.0 min hold) to 250 °C at 15°/min and then to 350 °C (28 min hold) at 15°/min. The carrier gas was He at a constant flow rate and we tested the effects of different flow rate from 1.0 to 2.4 ml/min. The FID was operated at 260 °C with 30 ml/min N_2 makeup gas. The mass spectrometers were operated in full scan mode over 50–750 amu. The MS transfer line temperature was held at 320 °C and the ion source temperature at 225 °C.

To assist with the identification of several unknown BHPs, selected extracts were also analyzed using an Agilent 6890 GC instrument coupled to a Waters GCT Premier TOF mass spectrometer for accurate mass determination. GC conditions, injector and column were identical to those above. Mass spectra were collected over a range of *m/z* 0–1000 using perfluorinated tributylamine as mass calibrant. This system provides a resolution (M/ΔM) of 7000 at 600 amu with accuracy better than 10 ppm. Analytes were identified on the basis of comparison of retention times and mass spectra (Section 3).

2.4. LC–MS

The acetylated TLEs were also analyzed using LC–MS with a 1200 Series HPLC instrument (Agilent Technologies) equipped with an autosampler and a binary pump linked to a Q-TOF 6520 mass spectrometer (Agilent) via an APCI interface operated in positive ion mode. The procedure was adapted from Talbot et al. (2003a). A Poroshell 120 EC-C_{18} column (2.1 ×

150 mm, 2.7 μm; Agilent Technologies) at 30 °C was eluted isocratically first with MeOH/water (95:5, v:v; 2 min) at 0.15 ml/min, then with a linear gradient up to 20% (v) of isopropyl alcohol (IPA; 18 min at 0.19 ml/min) and finally isocratic for 10 min. The linear gradient was then set to 30% (v) IPA at 0.19 ml/min over 10 min (maintained for 5 min). The column was subsequently eluted using a linear gradient up to 80% IPA (v) over 1 min at 0.15 ml/min and isocratic for 14 min. Finally, the column was eluted with MeOH/water (95:5) at 0.15 ml/min for 5 min. The APCI parameters were: gas temperature 325 °C, vaporizer 350 °C, drying gas (N_2) 6 l/min, nebulizer (N_2) flow 30 l/min, capillary voltage 1200 V, corona needle 4 μA, fragmentor 150 V Data were recorded by scanning *m/z* 100–1600. Identification of hopanoids was achieved using exact mass data and comparison of retention times and mass spectra with published data (Talbot et al., 2003b, 2007).

3. Results and discussion

3.1. Hopanoid identification

A variety of triterpenoids with both hopanoid and gammacerane skeletons were identified in the extracts from *R. palustris* (Table 1). A typical chromatogram is shown in Fig. 1, although the presence and relative abundance of different triterpenoids varied substantially between cultures and conditions. Diplopterol (**IV**) and diploptene [hop-22(29)-ene, **II**] were assigned by comparison with extracts from *Methylococcus capsulatus*, a known producer of these compounds (Summons and Jahnke, 1992). Two isomers of diploptene, hop-17(21)-ene (**I**) and hop-21-ene (**III**), were assigned from the mass spectra of Ageta et al. (1987) and Summons and Jahnke (1992). These two isomers apparently derive mainly from dehydration of diplopterol during workup, because they are present in much lower abundance in the hydrocarbon fraction from silica gel column chromatography of the *R. palustris* extract prior to derivatization (Doughty et al., 2011). Tetrahymanol (**VIII**) was assigned by comparison with extracts from a culture of *Trimyema minutum* grown on *Methanococcus thermolithotrophicus* (Baumgartner et al., 2002). BHtetrol (**V**) was identified by comparison with the same compound in extracts from cultured *Phormidium luridum*. BHaminotriol (**VI**) was assigned from its mass spectrum under the assumption that it is the most abundant N-containing hopanoid in *R. palustris* (Talbot et al., 2003b). The 2-methyl homologs of many hopanoids were also observed, and could be assigned both from their characteristic retention time shift (ca. 0.2–0.5 min earlier on the DB-XLB column) and the change in major MS fragment from *m/z* 191 to 205. Localization of the methyl at C-2 had been confirmed in *R. palustris* by Rashby et al. (2007). A 20-methyl isomer of tetrahymanol was also tentatively assigned as largely coeluting with 2-methyltetrahymanol (Bravo et al., 2001). We have never observed an A-ring methylated BHaminotriol in *R. palustris*, nor have hop-17(21)-ene or hop-21-ene – when isolated using silica gel chromatography – been observed with A-ring methylation. The latter two compounds are commonly methylated at C-2 when found in total lipid extracts, consistent with their derivation primarily from the dehydration of diplopterol.

In acid hydrolyzed extracts, 32,35-anhydrobacteriohopanetetrol (**IX**) was found, together with its 2-methyl homolog. It was assigned by comparison with a published spectrum (Bednarczyk et al., 2005) and by the concomitant disappearance of the parent compound, BHtetrol (see Fig. 2; Schaeffer et al., 2008). Four other compounds, observed in different strains of *R. palustris* and on different columns, did not match with any reported spectra and we propose tentative structures as follows. BHP-550 (**X**) has a measured mass of 550.4363, giving a likely formula $C_{37}H_{58}O_3$ (550.4386), with 3 double bond equivalents (DBEs) in addition to the hopanoid rings. The peak disappears when the component is hydrolyzed or silylated, indicating a free OH group. The molecular weight of 550 thus pertains to the acetylated derivative. We propose a structure analogous to anhydroBHtetrol, but with a furan ring and single OH. However, a structure with two C=C bonds, one keto group and

one OH would also be compatible with the data. The compound appears to be a degradation product of BHaminotriol when run on the more polar DB-XLB column, as it does not appear during analysis with DB-1HT or DB-5HT columns. BHP-508 (**XI**) is similar, but with a measured mass of 508.4323, suggesting an elemental composition of $C_{35}H_{56}O_2$ (508.4280) with 3 DBEs in addition to the hopanoid rings. However, the peak does not shift when hydrolyzed or silylated, indicating no free OH (i.e. the molecular weight of 508 does not include an acetate derivative). We interpret the structure as being the keto tautomer of **X**, although again a structure with no ring and two keto groups could also be compatible. BHP-492 (**XII**) has a nominal mass of 492 (GC-TOF data not available) and was observed only in extracts from *R. palustris* strain DSM 123. Its structure can be parsimoniously explained as a single furan ring on the side chain, although this awaits confirmation. A small 2-methylated homolog was also observed, suggesting that BHaminotriol is not the parent compound. BHP-570 (**XIII**) has a nominal mass of 570 Da, shifts when silylated, and is most readily explained as the bacteriohopanediol (570 is the molecular weight of the di-acetylated derivative). It was observed only in extracts from *R. palustris* strain DSM 123 and no 2-methyl homolog was observed. Accurate mass was not obtained for either of the latter two compounds because they are rarely encountered. Annotated mass spectra and structures of these compounds are provided in Electronic Annex EA-1.

3.2. Optimization of sample preparation procedures

3.2.1. Hydrolysis—The total lipid extracts contain relatively large amounts of diacylglycerides, which elute between 27 and 33 min on the XLB column. Similar retention times were observed on other columns. To remove them, we employed hydrolysis under acidic (either AcCl or HCl aq.) or basic (NaOH) conditions, all at 1 M concentration, at a temperature from 60–80 °C and for 20 min to 12 h. While all of these procedures were effective in removing diacylglycerides, they also all led to significant analyte degradation, most notably the conversion of diplopterol (**IV**) to hopenes (**I–III**) and of BHtetrol (**V**) to anhydroBHtetrol (**IX**; Fig. 2). None of the methods tested were able to simultaneously remove diacylglycerides while preserving diplopterol and BHtetrol. Because the diacylglycerides fortuitously elute after tetrahymanol and before BHtetrol, in a region with few or no hopanoids, their presence does not significantly impact the analysis of hopanoids. We therefore recommend that, when assigning original hopanoid structures is of highest priority, hydrolysis of the lipid extract should be avoided. If hydrolysis of diacylglycerides is necessary, then our data indicate that hydrolysis with HCl leads to the least amount of hopanoid degradation.

3.2.2. Derivatization—Conditions for acetate formation were further optimized to provide quantitative derivatization while minimizing degradation of sensitive hopanoids (mainly diplopterol and BHtetrol). A single extract was split into multiple aliquots and derivatized with 1:1 Ac_2-O:pyridine at a temperature from 60–80 °C and time ranging from 5 min to overnight. Relative concentrations were calculated using FID peak areas relative to an internal standard. Maximal concentration of most hopanoids, including BHtetrol, was recovered with derivatization for 10–30 min and at 70 °C. Shorter reaction time (5–10 min) resulted in markedly loweryield of BHtetrol, but higher yield of hopenes. Evidently these compounds can be partially degraded under the derivatization conditions. Longer reaction time (> 30 min) resulted in a lower yield of all hopanoids. Efficiency was only weakly sensitive to temperature, but 70 °C was the optimum.

3.2.3. Comparison with oxidative cleavage—To provide quantitative comparison of our new approach with the commonly employed oxidative cleavage/hydride reduction method, we analyzed seven acetylated extracts using both methods. For each sample the TLE was split, with 90% processed via the oxidative cleavage method and the other 10%

derivatized directly with Ac_2O. Both sample sets were then analyzed at the same time using the same instrument conditions, and both were quantified using FID peak areas vs. an internal standard (epiandrosterone). To focus specifically on the efficiency of the polyol cleavage/reduction, we compared the abundance of BHtetrol (and 2-methylBHtetrol) from the HT–GC method with that of the C_{32} hopanol (and 2-methyl C_{32} hopanol) from oxidative cleavage (Table 2). One complication of this comparison is that BHaminotriol and adenosylhopane, both very abundant in *R. palustris*, will contribute to the C_{32} hopanol generated from oxidative cleavage, thus overestimating the efficiency of the oxidation procedure. To gain further insight into this issue, our dataset for the comparison included five different strains of *R. palustris*, grown under different conditions, which should have different relative abundances of extended BHPs.

The data in Table 2 indicate that the HT GC–MS method recovered 0.9–3.2× more BHtetrol than C_{32} hopanol and 1.9–6.9× more 2-methyl BHtetrol than 2-methyl C_{32} hopanol. Because BHaminotriol and adenosylhopane have never been observed with A-ring methylation in *R. palustris*, we interpret the results for 2-methyl BHPs to be the most representative comparison, i.e. the new HT–GC method has roughly 2–7× higher recovery than oxidative cleavage. Assuming that reaction does not alter the 2-methyl/desmethyl ratio of BHPs, we can further infer that about half of the C_{32} hopanol generated by this procedure is derived from BHaminotriol and adenosyl hopane. The question of why the relative recoveries of the two methods is so highly variable is difficult to answer, but comparison of data from different strains suggests that it is not biologic, as follows. The ratios of BHtetrol/C_{32} hopanol and 2-meBHtetrol/2-meC_{32} hopanol are highly correlated across our entire sample set (R^2 0.82). A strong correlation would not be expected if the variability were due to differing abundances of BHtetrol, BHaminotriol and adenosylhopane, but is entirely consistent with variable loss of all BHPs in the oxidative cleavage procedure. It appears likely then that the yield from the oxidative cleavage procedure is not only low (15–50%) but also quite variable.

3.3. Column selection

A minimum criterion for suitable GC columns is the ability to elute the tetraacetate derivative of BHtetrol (MW 715), with good peak shape and in reasonable time. We tested three columns that met this criterion: DB-XLB, DB-5HT and DB-1HT (all 30 m). A film thickness of 0.10 μm or less was required for BHtetrol to elute at 350 °C. We also tested a thicker (0.25 μm) film DB-XLB column but BHtetrol did not elute. There are several tradeoffs between the choices of stationary phase (Fig. 3). With the DB-1HT column, BHaminotriol eluted without apparent degradation, but there was virtually no separation between any 2-methyl/desmethyl homologs.

In contrast, the DB-XLB column provided baseline separation (typically ca. 0.2 min for hopenes and 0.5 min for BHtetrol) between 2-methylBHPs and their desmethyl homologs, but was unable to elute BHaminotriol. Instead, chromatograms from the DB-XLB column included compounds BHP-550, BHP-508 and a poorly-shaped peak eluting immediately after BHtetrol (MW 653; Fig. 1). The same extract run on the DB-1HT column afforded BHaminotriol but not BHP-550 or BHP-508. We thus surmise that BHaminotriol (and possibly also adenosyl hopane, but not BHtetrol) breaks down on the moderately polar XLB stationary phase. This inference is strengthened by the observation that BHaminotriol, adenosyl hopane, BHP-550 and BHP-508 are never methylated at C-2 in *R. palustris*, whereas BHtetrol is.

A DB-5ms column provides good separation between 2-methyl/ desmethyl homologs, equivalent to that provided by DB-XLB, and can be a good choice for analysis of hopenes and hopanols. But with a maximum temperature of 340 °C, we were unable to recover

BHtetrol from this column. The related DB-5HT column chemistry has been used by Innes et al. (1997) and Blumenberg et al. (2006) for BHP analysis. While it is reported to have similar characteristics to DB-5ms, in practice it yielded essentially no separation of hopenes and 2-methylhopenes, and only partial separation of BHtetrol from 2-methylBHtetrol (Fig 3). The DB-5HT column is able to elute BHtetrol and BHaminotriol from *R. palustris* and is also reported to successfully elute BHpentol (H. Talbot, personal communication).

In summary, the analyst is left with two imperfect alternatives. DB-5HT columns provide the best recovery of polyfunctionalized BHPs, including those with amine groups, but do not provide good separation of 2-methyl/desmethyl homologs. Although the two can be distinguished by monitoring *m/z* 191 vs. 205, there are some problems with quantifying compounds in this way (Section 3.5.1). This column is to be preferred when observation of amino-functionalized BHPs is a priority. In contrast, DB-XLB columns do not elute BHaminotriol and larger hopanoids, but do provide baseline separation of the 2-methyl/ desmethyl homologs for all eluted BHPs. This is particularly valuable when accurate measurements of 2-methyl ratios are a priority, or for compound-specific isotope analysis where baseline separation is required. Because the current investigation was undertaken as part of a larger effort to understand hopanoid function and distribution in *R. palustris*, which makes abundant 2-methylBHPs, the DB-XLB column was used for most tests reported here.

3.4. Method optimization

GC conditions were optimized using a single extract from *R. palustris* strain BisA53, derivatized with Ac_2O and run repeatedly under systematically varied conditions. Maximum GC oven temperature, PTV injector temperature and column flow rate were all tested. The DB-XLB column was employed with the Caltech Trace-DSQ system for these tests.

Maximum programmed oven temperature was varied systematically from 300 to 360 °C in 10 °C increments, with a constant column flow rate of 1.3 ml/min and maximum PTV injector temperature of 325 °C. Results indicate that a minimum temperature of 340 °C was required to elute BHtetrol in < 1 h, and even at this temperature peak shape was poor (Fig 4). Retention time decreased, and peak shape improved, up to the maximum column temperature of 360 °C The 360 °C run also yielded a slightly larger peak for BHtetrol relative to other experiments, though this result was not replicated. Results at 350 °C were nearly as good as at 360 °C and should provide for longer column lifetime, so this temperature was adopted for subsequent measurements.

The maximum temperature of the PTV injector (i.e. “sample transfer temperature”) was varied between 250 and 350 °C in 25 °C increments, with a constant column flow rate of 1.3 ml/min and maximum oven temperature of 350 °C. Tests showed poor sample recovery at < 300 °C, but virtually identical results above 300 °C (data not shown). Peak area was marginally higher at 325 °C so we adopted this as our standard parameter, although any temperature between 300 and 350 °C would suffice. Increased degradation of diplopterol and/or BHtetrol at higher injector temperature was not observed. We further tested injection with a split/ splitless (S/SL) injector held at 300 °C using the same sample as for PTV injection. Using the S/SL injector, BHtetrol was eluted with good peak shape, but at only ca. 50% of the abundance with PTV injection. In contrast, the abundance of hopenes was similar with the two types of injector.

Carrier gas flow rate was varied at 1.0, 1.3, 1.6, 1.9 and 2.4 ml/ min, with maximum oven temperature 350 °C and injector temperature 325 °C. For all hopanoids, peak shape improved and retention time decreased up to the highest flow rate tested (data not shown). Adequate separation between the 2-methylhopanoids and desmethyl homologs was maintained even at 2.4 ml/min. However, for hop-21-ene and hop-22(29)-ene, which

substantially coelute, separation was noticeably worse at higher flow rate, and optimal separation of those isomers required lower (1.0–1.5 ml/ min) flow rate.

3.5. Quantification

3.5.1. Comparison of FID with MS—To assess the relative merits of various approaches to quantification, we grew and extracted a single large sample of *R. palustris* (TIE-1) under photoheterotrophic conditions. This particular culture produced large amounts of 2-methyl BHPs and no tetrahymanol, for unknown reasons. An internal standard (epiandrosterone) was added to the TLE, which was then serially diluted (1:3) 4×, resulting in a dilution series (designated D1–D5) spanning two decades of concentration. Each sample was derivatized with Ac_2O, then analyzed on two different columns (DB-XLB and DB-5HT) using two different detectors (MS and FID). Each analysis was performed in triplicate, with the resulting matrix representing 60 analyses. For each chromatogram, peaks corresponding to 9 separate hopanoids were integrated in three ways, using: (i) FID peak areas, (ii) TIC peak areas from MS, or (iii) SIM peak areas from *m/z* 191 for desmethyl and *m/z* 205 for 2-methyl hopanoids. Results from triplicate analyses were then averaged. The complete dataset is provided in Electronic Annex EA-2.

Several aspects of the dataset are highlighted in Table 3. Section A tabulates the ratio of FID peak areas for selected hopanoids vs. the internal standard (IS) at each dilution level. Because the IS was added prior to dilution, the ratio should theoretically remain the same at all dilution levels. Instead, for all samples the abundance of hopanoids relative to IS increased slightly over the first two dilutions, then decreased dramatically over the final two. The pattern is more severe for the polyfunctionalized hopanoids than for the hopenes; in the extreme case of BHaminotriol, the hopanoid/IS ratio changed from 3.4 for dilution 3 to 0.05 for dilution 5. The pattern is similar for both FID and MS data (not shown), suggesting that it arises during chromatography. The phenomenon is qualitatively consistent with preferential loss of hopanoids due to either adsorption or thermal decomposition and highlights the difficulty of achieving quantitative analysis of these high-boiling compounds.

Sections B and C of Table 3 document the quantitative response from MS relative to that from FID for the same hopanoids. The values were calculated as:

$$\text{Relative response} = \frac{\frac{A_{MS}}{IS_{MS}}}{\frac{A_{FID}}{IS_{FID}}}$$

where A and IS represent peak areas for the analyte and internal standard, respectively, and subscripts MS and FID represent peak areas obtained from MS (TIC or SIM) or FID data. By comparing peak areas between MS and FID data for the same sample, effects of analyte loss during chromatography (as discussed above) are avoided. In essence, these relative response factors represent the bias in concentration that would result from assuming a unit response factor for the MS, i.e. as is commonly done when authentic standards are not available. Using total ion counts (Table 3, section B) results in a relative response ranging from 0.25 to 1.3, with the lowest values for BHaminotriol and highest values for diplopterol. Response factor did not change systematically with dilution for the hopenes, but did decrease with dilution for the functionalized hopanoids. This pattern would be consistent with an increased loss of high molecular weight (MW) hopanoids in the MS transfer line and source relative to FID. When BHtetrol was quantified on both XLB and 5HT columns, the resulting response factors differed by 2-fold. These results were obtained roughly 2 weeks apart, with several source tunings between them, and presumably reflect inherent variability

in MS response factor. Quantitation using SIM chromatograms (*m/z* 191 and 205; Table 3, section C) resulted in similar patterns as for the TIC data, but with increased variability. In this case, response factors varied from 0.16 to 2.72. Our conclusion is that to achieve accurate quantitation using GC–MS, multi-point calibration curves are a necessity and TIC data are preferable to SIM data. Without them, estimated concentration may be in error by a factor of 3 or more.

Finally, we evaluated potential bias in calculated 2-methyl ratios for the three detection schemes (Table 3, section D). In doing so, we assumed that FID results were the most accurate, and so compared MS data against them. For all compounds, the 2-methyl ratios returned by TIC data are statistically indistinguishable from those from FID, consistent with virtually identical response factors between 2-methyl and desmethyl homologs of any given hopanoid structure. 2-methyl ratios derived from SIM data are significantly lower, however, typically by 20–30% (BHtetrol is the exception).This bias can be rationalized by the observation that *m/z* 191 is a larger peak than *m/z* 189 in the mass spectrum of most desmethyl BHPs, but *m/z* 205 is a smaller peak than *m/z* 189 for most 2-methyl BHPs.

3.5.2. Detection limit—Analytical bias notwithstanding, SIM analysis using *m/z* 191 and 205 chromatograms provides the most convenient and sensitive method for quantifying hopanoids of varying composition in an automated fashion. To assess detection limits using this approach, we used an *R. palustris* extract that had been quantified by GC-FID to generate a four point calibration curve. SIM analysis of the same extract then allowed us to calculate detection limit at a signal/ noise ratio of 10: hop-17(21)-ene, 34 pg; hop-22(29)-ene, 65 pg; hop-21-ene, 69 pg; tetrahymanol, 170 pg; BHP-550, 2.4 ng; BHP-508, 1.2 ng; BHtetrol, 0.97 ng. Detection limit for the 2-methyl homologs was similar.

3.5.3. Comparison with LC–MS—To further explore some of the advantages and disadvantages of high temperature GC–MS, we analysed the same dilution series of *R. palustris* extracts (Section 3.5.1) by LC–MS using a QTOF mass spectrometer. Although the functionalized hopanoids of *R. palustris* have been previously described (Rashby et al., 2007; Talbot et al., 2008), there has not been a direct comparison of quantitative GC–MS and LC–MS measurements on the same extract. Absolute concentration of hopanoids was calculated using FID peak areas relative to the epianderosterone internal standard for GC, and using *m/z* 191 or 205 peak areas relative to a 4 point calibration curve generated with an authentic standard of pregnone diacetate for LC, assuming unit response factor for all analytes (Sáenz et al., 2011).

The results (Table 4) indicate that LC–MS measured concentrations of BHtetrol, 2-meBHtetrol, and BHaminotriol that were 50–100% higher than the maximum values measured with GC–MS. The 2-methyl ratios were statistically indistinguishable between the two approaches. LC–MS concentrations did exhibit minor decreases with dilution level, but not nearly to the extreme that GC-FID concentrations did. Apparently analyte loss is much less severe in LC-based analyses. Our data do not allow us to distinguish whether the higher apparent concentrations measured with LC– MS reflect loss in the GC-FID approach, or a bias due to the assumption of equal response factors for hopanoids vs. pregnone diacetate in the LC–MS approach. In either case, it appears that the LC–MS concentration is at least within a factor of 2 (possibly much better) of being ‘correct’, and that the LC–MS technique is much less susceptible to loss of hopanoids at very low dilution. This method also provides the ability to quantify highly functionalized BHPs (such as adenosylhopane), which do not elute from HT–GC on any column we have tested, and so is complementary to HT GC–MS analysis.

3.6. Survey of R. palustris strains

As an initial demonstration of the optimized methodology, we measured the abundance of BHPs in six different strains of *R. palustris* grown under both heterotrophic and photoheterotrophic conditions (Table 5). All six strains were isolated from freshwater sediments with the 3 BisB strains and the HaA2 strain isolated simultaneously from the Netherlands (Oda et al., 2002; Jiao et al., 2005). All six strains have 16S rRNA sequence identity of 97% or greater and each of their genomes contain hopanoid biosynthesis genes required to produce both methylated and unmethylated hopanoids (Oda et al., 2008; Welander et al., 2012). Data for BHP-550 are compiled as a proxy for BHaminotriol, although the quantitative correspondence of the two compounds has not been verified. All cultures were harvested at mid-exponential phase.

The data in Table 5 demonstrate that all six strains produced the same set of hopanoids. However, there was significant variation in hopanoid abundance between strains and between photoautotrophic and heterotrophic conditions. The majority of strains tended to produce large amounts of hopenes under both growth conditions, with the exception of BisB5 having more tetrahymanol. All strains produced similar amounts of BHtetrol, with no significant difference between growth conditions. The 2-methyl ratio also varied significantly between strains; for example BisA53 gave a 2-methyl ratio of 0.1 whereas for BisB18 it was 5.9, both for diplopterol under photoheterotrophic conditions. Thus it seems that, despite the similarity in hopanoid biosynthetic gene sequences between these strains, as well as the similar environmental niche they inhabit, the production of certain hopanoids can vary quite substantially.

4. Conclusions

We present optimized procedures for the identification and quantitation of polyfunctionalized hopanoids using GC–MS with high-temperature, thin film columns. The method requires only acetylation of the total lipid extract, so is more rapid and efficient than the oxidative cleavage method. We show that hydrolysis of extracts leads to the generation of many artifactual hopanoid structures, several of which were tentatively identified based on accurate masses from GC-TOF-MS. DB-5HT type columns can successfully elute BHtetrol, BHpentol and BHaminotriol in < 1 h at a maximum oven temperature of 360 °C, but do not fully separate 2-methyl/desmethyl homologs. In contrast, DB-XLB columns do not elute BHpentol or BHaminotriol, but provide baseline separation of 2-methyl/desmethyl homologs. Quantification using either total ion counts, selected ions (*m/z* 191 and 205), or FID showed that the mass spectrometer exhibits strong (up to threefold) variation in relative response to different hopanoids, so FID provides the most accurate quantitation when authentic standards are not available. The ratio of 2-methyl to desmethyl BHPs determined from TIC of baseline-resolved peaks are similar to those from FID, but those determined from SIM analysis using *m/z* 205/ 191 are systematically low by 10–30% Quantitation of functionalized hopanoids with LC–MS using pregnone diacetate as a calibration standard yielded a concentration 50–100% higher than that measured from GC-FID, but the reasons for the discrepancy are not known.

Supplementary Material

Refer to Web version on PubMed Central for supplementary material.

Acknowledgments

Research at Caltech was supported by Grants from the NASA Exobiology program (NNX07AN49G and NNX12AD93G) to A.L.S. and D.K.N. Research at MIT was supported by Grants from the NSF Program on

Emerging Trends in Biogeochemical Cycles (OCE-0849940), the NASA Astrobiology Institute, and a NASA Postdoctoral Program Fellowship to P.V.W. D.K.N. is an Investigator of the Howard Hughes Medical Institute. We thank M. Blumenberg and M. Elvert for constructive reviews of the manuscript.

Appendix A. Structures described in text

See Fig. A1.

Appendix B. Supplementary material

Supplementary data associated with this article can be found, in the online version, at http://dx.doi.org/10.1016/j.orggeochem.2012.12.009.

Associate Editors—**H.M. Talbot** and **B. van Dongen**

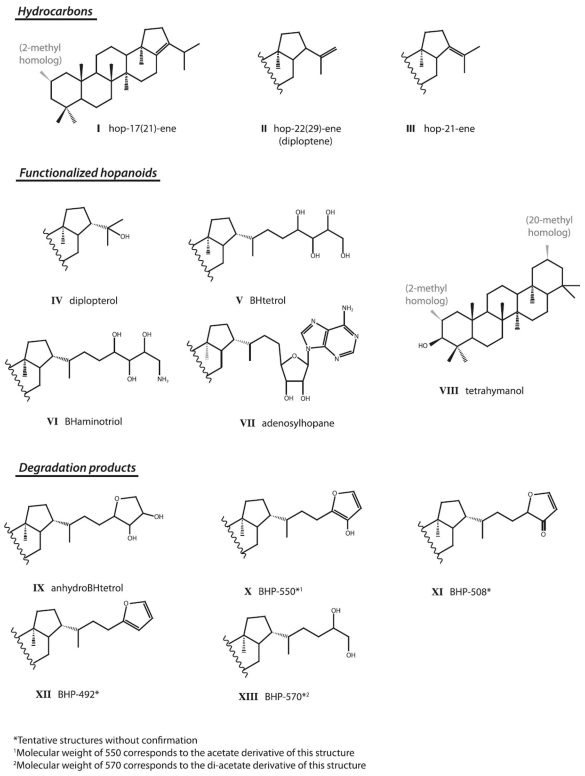

Fig. A1. Structures.

References

Ageta H, Shiojima K, Arai Y. Acid-induced rearrangement of triterpenoid hydrocarbons belonging to the hopane and migrated hopane series. Chemical and Pharmaceutical Bulletin. 1987; 35:2705–2716.

Baumgartner M, Stetter KO, Foissner W. Morphological, small subunit rRNA, and physiological characterization of *Trimyema minutum* (Kahl, 1931), an anaerobic ciliate from submarine hydrothermal vents growing from 28°C to 52°C. Journal of Eukaryotic Microbiology. 2002; 49:227–238. [PubMed: 12120988]

Bednarczyk A, Carillo Hernandez T, Schaeffer P, Adam P, Talbot HM, Farrimond P, Riboulleau A, Largeau C, Derenne S, Rohmer M, Albrecht P. 32,35-Anhydrobacteriohopanetetrol: an unusual bacteriohopanepolyol widespread in recent and past environments. Organic Geochemistry. 2005; 36:673–677.

Bligh E, Dyer W. A rapid method of total lipid extraction and purification. Canadian Journal of Biochemistry and Physiology. 1959; 37:911–917. [PubMed: 13671378]

Blumenberg M, Kruger M, Nauhaus K, Talbot H, Oppermann B, Seifert R, Pape T, Michaelis W. Biosynthesis of hopanoids by sulfate-reducing bacteria (genus *Desulfovibrio*). Environmental Microbiology. 2006; 8:1220–1227. [PubMed: 16817930]

Bradley AS, Pearson A, Sáenz JP, Marx CJ. Adenosylhopane: the first intermediate in hopanoid side chain biosynthesis. Organic Geochemistry. 2010; 41:1075–1081.

Brassell SC, Eglinton G, Maxwell JR. The geochemistry of terpenoids and steroids. Biochemical Society Transactions. 1983; 11:575–586. [PubMed: 6642066]

Bravo J, Perzl M, Hartner T, Kannenberg E, Rohmer M. Novel methylated triterpenoids of the gammacerane series from the nitrogen-fixing bacterium *Bradyrhizobium japonicum* USDA 110. European Journal of Biochemistry. 2001; 268:1323–1331. [PubMed: 11231284]

Brocks, JJ.; Summons, RE.; Schlesinger, W.; Holand, H.; Turekian, K. Sedimentary hydrocarbons, biomarkers for early life. In: Schlesinger, WH., editor. Treatise on Geochemistry Biogeochemistry. Vol. 8. Amsterdam: Elsevier; 2003. p. 63-116.

Doughty DM, Hunter RC, Summons RE, Newman DK. 2-Methylhopanoids are maximally produced in akinetes of *Nostoc punctiforme:* geobiological implications. Geobiology. 2009; 7:524–532. [PubMed: 19811542]

Doughty DM, Coleman ML, Hunter RC, Sessions AL, Summons RE, Newman DK. The RND-family transporter, HpnN, is required for hopanoid localization to the outer membrane of *Rhodopseudomonas palustris* TIE-1. Proceedings of the National Academy of Sciences USA. 2011; 108:E1045–E1051.

Farrimond P, Head I, Innes H. Environmental influence on the biohopanoid composition of recent sediments. Geochimica et Cosmochimica Acta. 2000; 64:2985–2992.

Farrimond P, Talbot H, Watson D, Schulz L, Wilhelms A. Methylhopanoids: molecular indicators of ancient bacteria and a petroleum correlation tool. Geochimica et Cosmochimica Acta. 2004; 68:3873–3882.

Fischer WW, Pearson A. Hypotheses for the origin and early evolution of triterpenoid cyclases. Geobiology. 2007; 5:19–34.

Fischer WW, Summons RE, Pearson A. Targeted genomic detection of biosynthetic pathways: anaerobic production of hopanoid biomarkers by a common sedimentary microbe. Geobiology. 2005; 3:33–40.

Flesch G, Rohmer M. Prokaryotic hopanoids: the biosynthesis of the bacteriohopane skeleton. European Journal of Biochemistry. 1988; 175:405–411. [PubMed: 3136017]

Innes H, Bishop A, Head I, Farrimond P. Preservation and diagenesis of hopanoids in recent lacustrine sediments of Priest Pot, England. Organic Geochemistry. 1997; 26:565–576.

Jiao Y, Kappler A, Croal L, Newman D. Isolation and characterization of a genetically tractable photoautotrophic Fe(II)-oxidizing bacterium, *Rhodopseudomonas palustris* Strain TIE-1. Applied and Environmental Microbiology. 2005; 71:4487–4496. [PubMed: 16085840]

Kannenberg E, Poralla K. Hopanoid biosynthesis and function in bacteria. Naturwissenschaften. 1999; 86:168–176.

Ochs D, Kaletta C, Entian K, Becksickinger A, Poralla K. Cloning, expression, and sequencing of squalene-hopene cyclase, a key enzyme in triterpenoid metabolism. Journal of Bacteriology. 1992; 174:298–302. [PubMed: 1729216]

Oda Y, Wanders W, Huisman LA, Meijer WG, Gottschal JC, Forney LJ. Genotypic and phenotypic diversity within species of purple nonsulfur bacteria isolated from aquatic sediments. Applied and Environmental Microbiology. 2002; 68:3467–3477. [PubMed: 12089030]

Oda Y, Larimer FW, Chain PSG, Malfatti S, Shin MV, Vergez LM, Hauser L, Land ML, Braatsch S, Beatty JT, Pelletier DA, Schaefer AL, Harwood CS. Multiple genome sequences reveal adaptations of a phototrophic bacterium to sediment microenvironments. Proceedings of the National Academy of Sciences USA. 2008; 105:18543–18548.

Ourisson G, Albrecht P. Hopanoids. 1. Geohopanoids: the most abundant natural products on Earth? Accounts of Chemical Research. 1992; 25:398–402.

Ourisson G, Albrecht P, Rohmer M. The Hopanoids: Palaeochemistry and biochemistry of a group of natural products. Pure and Applied Chemistry. 1979; 51:709–729.

Peters KE, Moldowan JM. Effects of source, thermal maturity, and biodegradation on the distribution and isomerization of homohopanes in petroleum. Organic Geochemistry. 1991; 17:47–61.

Peters, KE.; Walters, CC.; Moldowan, JM. The Biomarker Guide. second. Cambridge: Cambridge University Press; 2005.

Rashby SE, Sessions AL, Summons RE, Newman DK. Biosynthesis of 2-methylbacteriohopanepolyols by an anoxygenic phototroph. Proceedings of the National Academy of Sciences USA. 2007; 104:15099–15104.

Rohmer, M. Hopanoids. In: Timmis, KN., editor. Handbook of Hydrocarbon and Lipid Microbiology. Springer: Berlin Heidelberg; 2010. p. 133-142.

Rohmer M, Bouvier-navé P, Ourisson G. Distribution of hopanoid triterpenes in Prokaryotes. Journal of General Microbiology. 1984; 130:1137–1150.

Sáenz JP, Eglinton TI, Summons RE. Abundance and structural diversity of bacteriohopanepolyols in suspended particulate matter along a river to ocean transect. Organic Geochemistry. 2011; 42:774–780.

Schaeffer P, Schmitt G, Adam P, Rohmer M. Acid-catalyzed formation of 32,35-anhydrobacteriohopanetetrol from bacteriohopanetetrol. Organic Geochemistry. 2008; 39:1479–1482.

Seifert WK, Moldowan JM. The effect of thermal stress on source-rock quality as measured by hopane stereochemistry. Physics and Chemistry of the Earth. 1980; 12:229–237.

Summons RE, Jahnke LL. Identification of the methylhopanes in sediments and petroleum. Geochimica et Cosmochimica Acta. 1990; 54:247. [PubMed: 11537193]

Summons, RE.; Jahnke, LL. Hopenes and hopanes methylated in ring-A: correlation of the hopanoids of extant methylotrophic bacteria with their fossil analogues. In: Moldowan, JM.; Albrecht, P.; Philp, RP., editors. Biomarkers in Sediments and Petroleum. New Jersey: Prentice Hall; 1992. p. 182-200.

Summons RE, Jahnke L, Roksandic Z. Carbon isotopic fractionation in lipids from methanotrophic bacteria: relevance for interpretation of the geochemical record of biomarkers. Geochimica et Cosmochimica Acta. 1994; 58:2853–2863. [PubMed: 11540111]

Summons RE, Jahnke L, Hope J, Logan G. 2-Methylhopanoids as biomarkers for cyanobacterial oxygenic photosynthesis. Nature. 1999; 400:554–557. [PubMed: 10448856]

Talbot HM, Farrimond P. Bacterial populations recorded in diverse sedimentary biohopanoid distributions. Organic Geochemistry. 2007; 38:1212–1225.

Talbot H, Watson D, Murrell J, Carter J, Farrimond P. Analysis of intact bact high-performance eriohopanepolyols from methanotrophic bacteria by reversed-phase liquid chromatography-atmospheric pressure chemical ionisation mass spectrometry. Journal of Chromatography A. 2001; 921:175–185. [PubMed: 11471801]

Talbot H, Squier A, Keely B, Farrimond P. Atmospheric pressure chemical ionisation reversed-phase liquid chromatography/ion trap mass spectrometry of intact bacteriohopanepolyols. Rapid Communications in Mass Spectrometry. 2003a; 17:728–737. [PubMed: 12661028]

Talbot H, Summons RE, Jahnke L, Farrimond P. Characteristic fragmentation of bacteriohopanepolyols during atmospheric pressure chemical ionisation liquid chromatography/ion trap mass spectrometry. Rapid Communications in Mass Spectrometry. 2003b; 17:2788–2796. [PubMed: 14673828]

Talbot H, Watson D, Pearson E, Farrimond P. Diverse biohopanoid compositions of non-marine sediments. Organic Geochemistry. 2003c; 34:1353–1371.

Talbot H, Rohmer M, Farrimond P. Rapid structural elucidation of composite bacterial hopanoids by atmospheric pressure chemical ionisation liquid chromatography/ion trap mass spectrometry. Rapid Communications in Mass Spectrometry. 2007; 21:880–892. [PubMed: 17294511]

Talbot H, Summons RE, Jahnke L, Cockell C, Rohmer M, Farrimond P. Cyanobacterial bacteriohopanepolyol signatures from cultures and natural environmental settings. Organic Geochemistry. 2008; 39:232–263.

Welander PV, Hunter RC, Zhang L, Sessions AL, Summons RE, Newman DK. Hopanoids play a role in membrane integrity and pH homeostasis in *Rhodopseudomonas palustris* TIE-1. Journal of Bacteriology. 2009; 191:6145–6156. [PubMed: 19592593]

Welander PV, Coleman ML, Sessions AL, Summons RE, Newman DK. Identification of a methylase required for 2-methylhopanoid production and implications for the interpretation of sedimentary hopanes. Proceedings of the National Academy of Sciences USA. 2010; 107:8537–8542.

Welander PV, Doughty DM, Wu CH, Mehay S, Summons RE, Newman DK. Identification and characterization of *Rhodopseudomonas palustris* TIE-1 hopanoid biosynthesis mutants. Geobiology. 2012; 10:163–177. [PubMed: 22221333]

Wendt K, Lenhart A, Schulz G, Feil C. Crystallization and preliminary X-ray crystallographic analysis of squalene-hopene cyclase from Alicyclobacillus acidocaldarius. Protein Science. 1997; 6:722–724. [PubMed: 9070455]

Wendt K, Lenhart A, Schulz G. The structure of the membrane protein squalene-hopene cyclase at 2.0 angstrom resolution. Journal of Molecular Biology. 1999; 286:175–187. [PubMed: 9931258]

Zundel M, Rohmer M. Hopanoids of the methylotrophic bacteria *Methylococcus capsulatus* and *Methylomonas* sp. as possible presursors of C_{29} and C_{30} hopanoid chemical fossils. FEMS Microbiology Letters. 1985a; 28:61–64.

Zundel M, Rohmer M. Prokaryotic triterpenoids. 3. The biosynthesis of 2 β-methylhopanoids and 3 β-methylhopanoids of *Methylobacterium organophilum* and *Acetobacter pasteurianuss* sp. pasteurianus. European Journal of Biochemistry. 1985b; 150:35–39. [PubMed: 3926496]

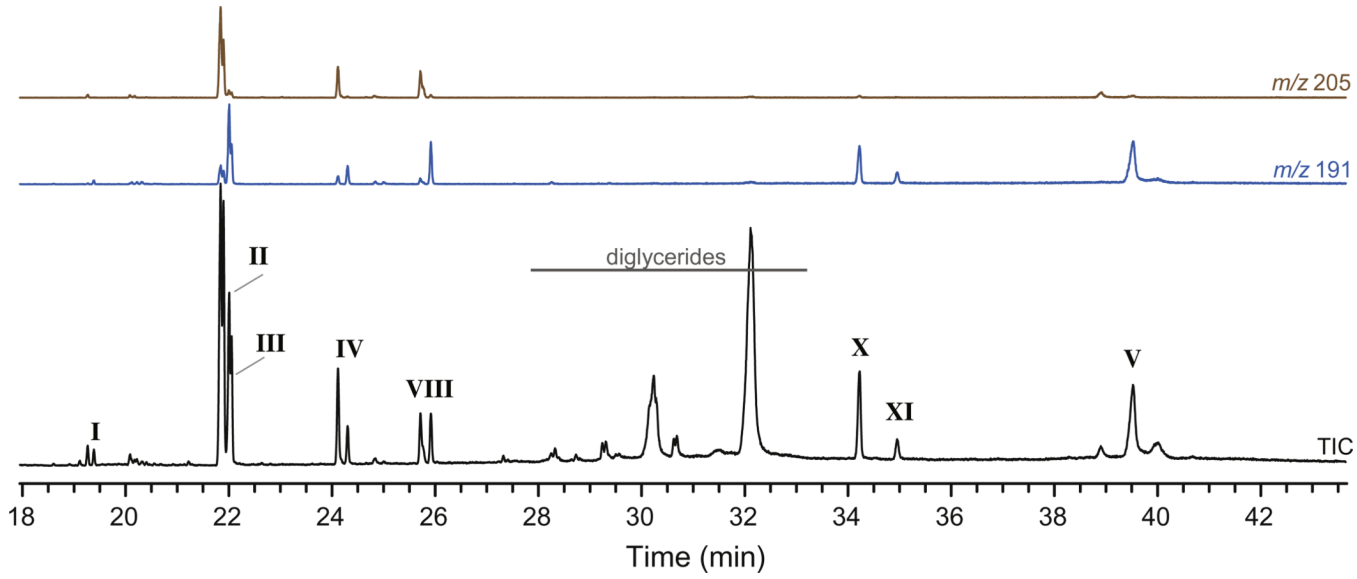

Fig. 1.

Typical GC–MS chromatogram of acetylated total lipid extract from *R. palustris* (strain TIE-1, grown photoautotrophically). Main hopanoid peaks are labeled. 2-Methyl homologs elute 0.2–0.5 min earlier on this column (DB-XLB) and are easily recognized in the *m/z* 205 trace. Note that compounds X and XI do not have 2-methyl homologs. The 2-methylhopenes are suspected to derive from dehydration of 2-methyldiplopterol, rather than de novo biosynthesis.

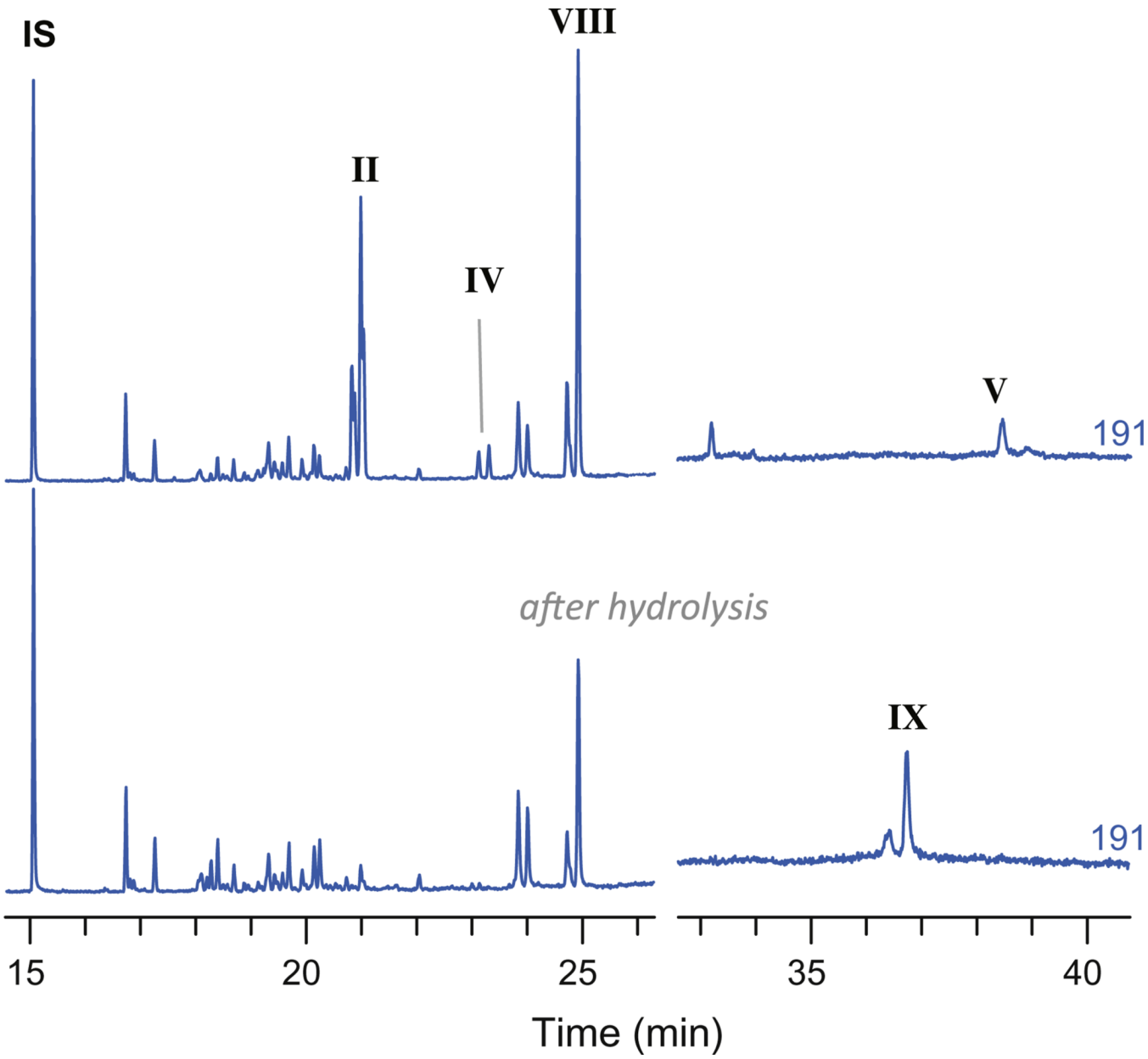

Fig. 2.

Chromatograms (*m/z* 191) of two aliquots from the same extract of *R. palustris* TIE-1, illustrating detrimental effect of hydrolysis. The upper chromato-gram reflects the extract treated only with Ac_2O, the lower chromatogram includes hydrolysis in MeOH/AcCl for 4 h at 80 °C. Hydrolysis leads to rearrangement of hop-21-ene to other isomers and nearly complete degradation of diplopterol (**IV**) and BHtetrol (**V**).

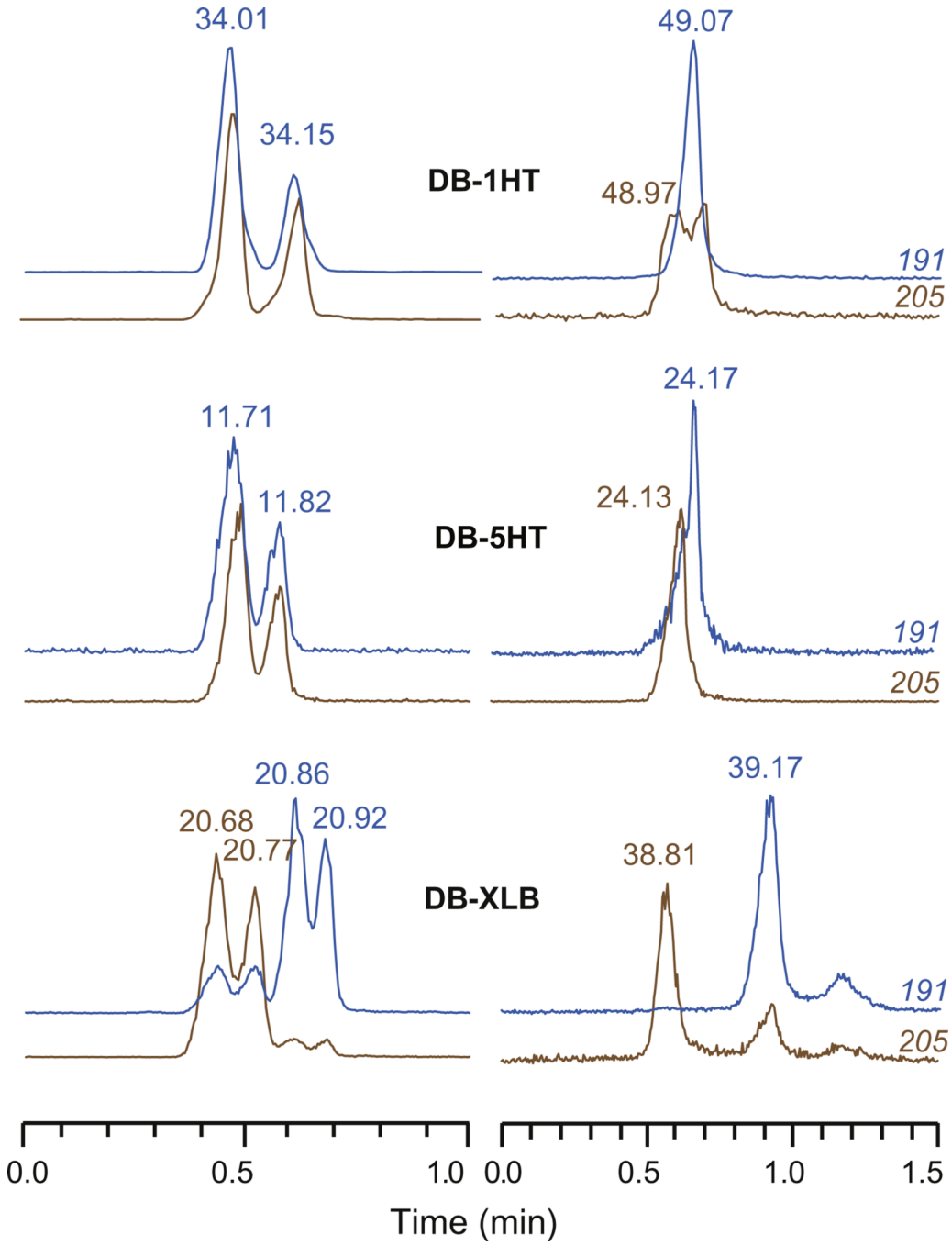

Fig. 3.

Partial GC–MS chromatograms (blue, *m/z* 191; brown, *m/z* 205) of acetylated extract from *R. palustris* TIE-1 analyzed with DB-1HT, −5HT, and –XLB columns of same dimensions, showing differences in separation for hopenes and BHtetrol. Data were collected with the same GC oven ramp rate. Peaks are shifted horizontally for comparison, actual retention times are given above selected peaks.

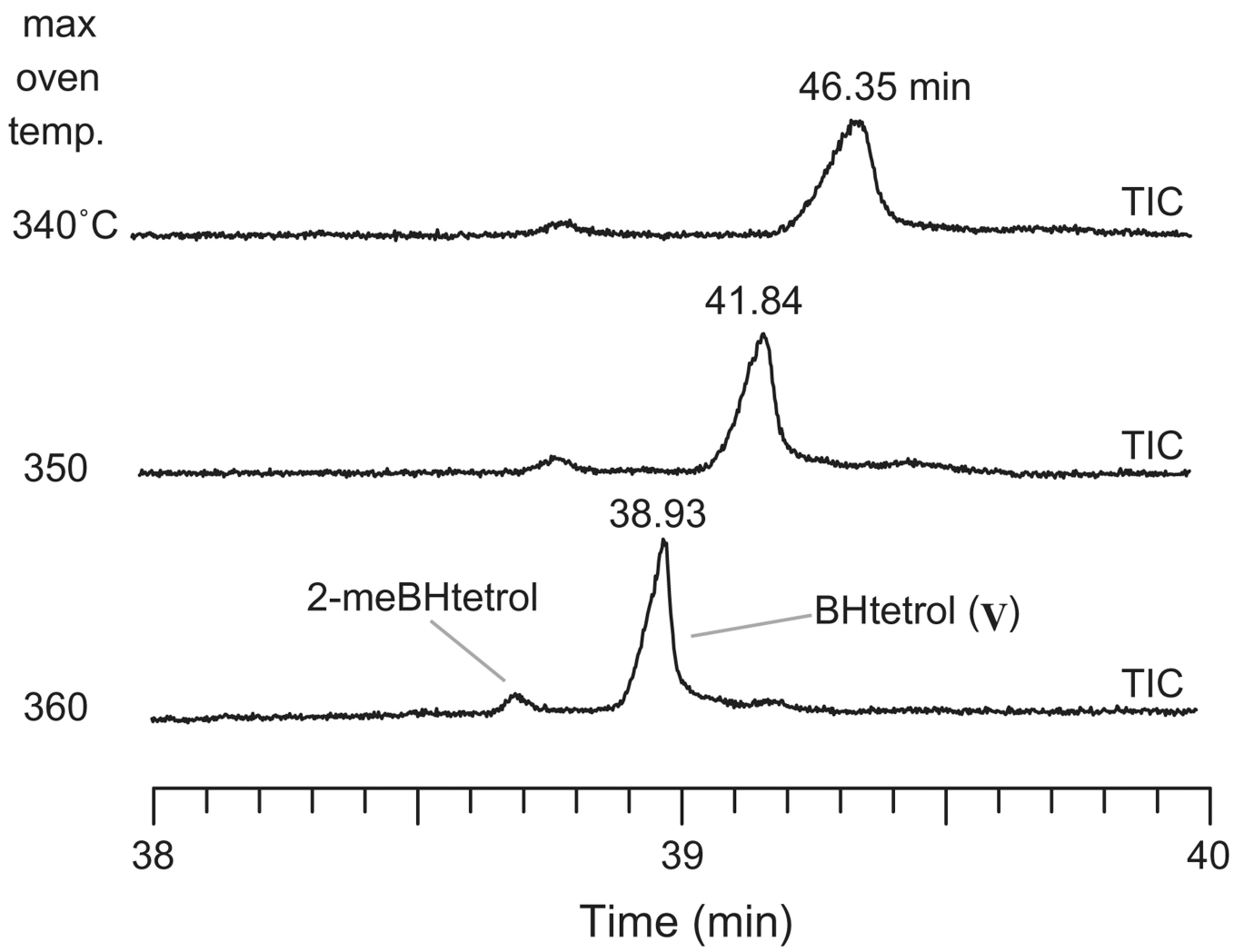

Fig. 4.

Comparison of peak shape and retention time for BHtetrol and 2-methyl BHtetrol with maximum oven program temperature. All runs used a 325 °C PTV injector, 1.3 ml/min flow rate, and DB-XLB column. TIC traces are plotted, with oven temperature indicated to left and retention time (min) above each trace. The upper two traces are shifted left for comparison, but all retain the same *x*-axis scaling such that peak width can be compared directly.

Table 1

Hopanoids in acetylated total lipid extracts from *R. palustris*.

Compound	Common Name	Structure	Rt (min)[a]	KI[b]	Diagnostic ions (*m/z*)
Hydrocarbons					
2-Methylhop-17(21)-ene			21.84	3123	424, 381, 245, 205, 161, 135
Hop-17(21)-ene		I	22.01	3134	410, 367, 231, 191, 161, 135
2-Methylhop-22(29)-ene			21.84	3361	424, 313, 205, 189, 95
Hop-22(29)-ene	Diploptene	II	22.01	3375	410, 299, 191, 189, 95
2-Methylhop-21-ene			21.90	3367	424, 381, 355, 245, 205, 189, 121
Hop-21-ene		III	22.05	3379	410, 367, 341, 231, 191, 189, 121
Functionalized lipids					
2-Methylhopan-22-ol			24.11	3566	442, 409, 205, 189, 149, 95
Hopan-22-ol	Diplopterol	IV	24.30	3584	428, 395, 191, 189, 149, 95
2-Methyltetrahymanol			25.71	3719	484, 424, 249, 205, 189, 83
20-Methyltetrahymanol			25.76	3724	NA[d]
Tetrahymanol	Tetrahymanol	VIII	25.92	3738	470, 410, 249, 191, 189, 69
2-Methylbacteriohopanetetrol			38.90	4877	728, 669, 493, 383, 205, 95
Bacteriohopanetetrol	BHtetrol	V	39.52	4920	714, 655, 493, 369, 191, 95
Bacteriohopaneaminotriol	BHaminotriol	VI	NA[c]	NA[c]	713, 654, 639, 492, 432, 369, 191
Adenosylhopane		VII	NA[e]	NA[e]	
Degradation products					
32,35-Anhydrobacteriohopane-tetrol	AnhydroBHtetrol	IX	38.40	NA	
BHP-550		X	34.23	4483	550, 493, 369, 329, 287, 191, 111
BHP-508		XI	34.95	4554	508, 493, 369, 287, 213, 191, 111
BHP-492	BHfuran	XII	30.26		492, 369, 271, 191, 81
Bacteriohopanediol	BHdiol	XIII	38.47		570, 369, 349, 191, 95

[a] Measured on 30 m DB-XLB column with conditions described in Section 2.2.

[b] Kovats retention index on DB-XLB column with conditions described in Section 2.2.

[c] BHaminotriol degrades on DB-XLB column and does not elute.

[d] Clean mass spectrum not obtained because of coelution with much more abundant 2-methyl isomer.

[e] Not observed in GC–MS due to high polarity.

Table 2

Comparison of hopanoid concentrations measured from direct acetylation vs. oxidative cleavage.

Strain	Growth condition	Desmethyl			2-Methyl		
		BHT (μg/mg)	C_{32} hopanol (μg/mg)	Ratio	2-meBHT (μg/mg)	2-me C_{32} hopanol (μg/mg)	Ratio
TIE-1	Heterotrophic	1.15	1.27	0.9	nd	0.019	
BisB5	Heterotrophic	0.83	0.79	1.1	0.25	0.075	3.3
BisB18	Heterotrophic	0.29	0.22	1.3	nd	0.003	
CGA009	Heterotrophic	0.52	0.45	1.2	0.07	0.020	3.4
HaA2	Heterotrophic	0.71	0.74	1.0	0.08	0.039	1.9
TIE-1	Photoheterotrophic	0.46	0.24	1.9	0.05	0.008	6.1
BisB5	Photoheterotrophic	0.77	0.24	3.2	0.08	0.012	6.9
	Avg.	0.68	0.56	1.5	0.10	0.025	4.3

Table 3

Comparison of hopanoid quantitation from MS and FID (ND, not detected).

	Diploptene	Hop-21-ene	Diplopterol	BHtetrol		Aminotriol
Method[a]	**GC/XLB**	**GC/XLB**	**GC/XLB**	**GC/XLB**	**GC/5HT**	**GC/5HT**
A. FID peak area ratio (hopanoid/IS)						
D1[c]	0.74 (0.03)[b]	0.23 (0.02)	0.03 (0.01)	0.77 (0.05)	5.84 (2.55)	0.96 (0.41)
D2	1.10 (0.28)	0.33 (0.07)	0.06 (0.02)	1.29 (0.25)	11.71 (4.22)	2.20 (0.83)
D3	0.93 (0.02)	0.31 (0.02)	0.09 (0.00)	1.13 (0.04)	15.21 (0.39)	3.42 (0.27)
D4	0.50 (0.02)	0.19 (0.01)	0.02 (0.00)	0.44 (0.01)	6.10 (0.27)	0.71 (0.08)
D5	0.27 (0.02)	0.20 (0.02)	ND	0.05 (0.02)	1.99 (0.17)	0.05 (0.02)
B. Relative response factor (TIC/FID)						
D1	0.89 (0.07)	0.94 (0.13)	2.05 (0.49)	1.17 (0.07)	0.66 (0.24)	0.39 (0.14)
D2	0.70 (0.17)	0.75 (0.13)	1.12 (0.27)	0.80 (0.14)	0.18 (0.05)	0.11 (0.02)
D3	0.60 (0.03)	0.53 (0.04)	1.17 (0.16)	0.69 (0.10)	0.07 (0.01)	ND
D4	0.80 (0.04)	0.89 (0.06)	0.87 (0.26)	0.50 (0.09)	ND	ND
D5	0.86 (0.08)	1.11 (0.11)	ND	ND	ND	ND
Mean	0.77	0.84	1.30	0.79	0.30	0.25
C. Relative response factor (SIM/FID)						
D1	1.65 (0.12)	1.11 (0.18)	3.60 (0.90)	2.05 (0.19)	1.57 (0.57)	0.24 (0.08)
D2	1.62 (0.39)	1.21 (0.21)	2.92 (0.74)	1.80 (0.36)	0.29 (0.08)	0.08 (0.02)
D3	1.34 (0.11)	0.87 (0.07)	2.86 (0.48)	1.28 (0.22)	0.13 (0.03)	ND
D4	1.48 (0.05)	1.50 (0.28)	1.51 (0.17)	0.67 (0.15)	ND	ND
D5	1.42 (0.12)	1.34 (0.16)	ND	ND	ND	ND
Mean	1.50	1.21	2.72	1.45	0.66	0.16
D. 2-Methyl ratio (2-me/desme)						
FID	2.64 (0.11)	6.15 (0.89)	6.20 (0.21)	4.20 (0.55)	NA[d]	NA[d]
TIC	2.53 (0.20)	5.83 (1.23)	6.82 (1.21)	3.87 (0.55)	NA[d]	NA[d]
SIM	2.24 (0.25)	4.44 (0.74)	5.44 (1.02)	4.69 (1.01)	3.30 (1.15)	NA[d]

[a] Analysis method and column used (either DB-XLB or DB-5HT).

[b] Each entry represents the mean of three replicate analyses, with 1 standard deviation in parentheses.

[c] D1–D5 indicate the five serial 1:3 dilutions of the same sample; relative abundances: D1 100%, D2 33%, D3 11%, D4 3.7%, D5 1.2%.

[d] Not applicable; 2-methyl and desmethyl homologs not adequately separated on the DB-5HT column.

Table 4

Comparison of hopanoid quantitation from GC-FID and LC–MS.

	BHtetrol		2MeBHtetrol		BHaminotriol		Adenosyl hopane
Method[a]	**GC/XLB**	**LC**	**GC/XLB**	**LC**	**GC/5HT**	**LC**	**LC**
D1[c]	5.8[b]	13.8	24.2	59.9	7.2	50.4	7.1
D2	9.7	13.4	38.4	56.1	16.5	49.0	6.1
D3	8.5	12.0	33.3	52.8	25.7	44.6	6.2
D4	3.3	12.8	12.5	44.5	5.3	38.3	6.0
D5	0.3	9.5	1.8	29.6	0.4	20.5	0.8
Mean	5.5	12.3	22.0	48.6	11.0	40.6	5.2

[a] Analysis method and column (either DB-XLB or DB-5HT).

[b] Each entry represents the mean of three replicate analyses; units are ng hopanoid/μg total lipid.

[c] D1–D5 indicate the five serial 1:3 dilutions of the same sample; relative abundance: D1 100%, D2 33%, D3 11%, D4 3.7%, D5 1.2%.

Table 5

Hopanoid concentration and 2-methyl ratio for 6 strains of *R. palustris*.

	TIE-1		CGA009		BisA53		BisB5		BisB18		HaA2	
	H[a]	PH[b]	H	PH	H	PH	H	PH	H	PH	H	PH
Concentration (μg/mg dry wt.)												
Hop-17(21)-ene	0.09	0.04	0.05	0.06	0.04	0.22	0.09	0.08	0.15	0.10	0.19	0.11
Hop-22(29)-ene + hop-21-ene	3.11	1.18	1.03	0.74	2.71	3.19	1.05	0.38	3.98	0.62	4.26	2.33
Diplopterol	0.58	0.44	0.14	0.10	0.30	0.21	0.37	0.06	1.06	0.12	0.77	0.85
Tetrahymanol	0.07	0.21	0.37	0.88	1.02	0.27	2.88	3.59	0.31	0.24	2.34	0.34
BHP-550	0.44	0.46	0.20	0.21	nd	0.14	0.74	0.67	0.04	0.23	0.59	0.35
BHtetrol	0.34	0.25	0.29	0.38	0.70	0.38	0.34	0.34	0.40	0.23	0.91	0.34
2-Methyl ratio												
Hop-17(21)-ene	0.4	0.8	1.1	1.6	0.4	0.1	0.4	0.7	0.5	2.5	0.3	0.1
Hop-22(29)-ene + hop-21-ene	0.3	0.8	1.2	2.2	0.2	0.1	0.8	1.2	0.5	4.3	0.4	0.0
Diplopterol	0.7	1.1	3.8	4.2	0.6	0.1	1.5	2.5	0.9	5.9	0.7	0.0
Tetrahymanol	0.5	0.6	2.3	1.0	0.8	2.8	1.6	0.9	0.9	5.9	1.0	0.0
BHP-550	0.0	0.0	0.0	0.0	0.0	0.0	0.0	0.0	0.0	0.0	0.0	0.0
BHtetrol	na	0.09	0.20	0.19	0.10	0.25	0.41	0.11	0.16	0.52	0.09	Na

[a]Growth under heterotrophic conditions.

[b]Growth under photoheterotrophic conditions.